



PHIL Inverter Test Report

Analysis of High-Penetration Levels of PV into the Distribution Grid in California

March 12 — March 16, 2012

Matt Kromer
Satcon Technology Corporation
Boston, Massachusetts

NREL Technical Monitor: Barry Mather

**NREL is a national laboratory of the U.S. Department of Energy
Office of Energy Efficiency & Renewable Energy
Operated by the Alliance for Sustainable Energy, LLC.**

This report is available at no cost from the National Renewable Energy
Laboratory (NREL) at www.nrel.gov/publications.

Subcontract Report
NREL/SR-5500-57786
June 2013

Contract No. DE-AC36-08GO28308

PHIL Inverter Test Report

Analysis of High-Penetration Levels of PV into the Distribution Grid in California

March 12 — March 16, 2012

Matt Kromer
Satcon Technology Corporation
Boston, Massachusetts

NREL Technical Monitor: Barry Mather
Prepared under Subcontract No. LAT-2-11815-01

**NREL is a national laboratory of the U.S. Department of Energy
Office of Energy Efficiency & Renewable Energy
Operated by the Alliance for Sustainable Energy, LLC.**

This report is available at no cost from the National Renewable Energy
Laboratory (NREL) at www.nrel.gov/publications.

**This publication was reproduced from the best available copy
submitted by the subcontractor and received no editorial review at NREL.**

NOTICE

This report was prepared as an account of work sponsored by an agency of the United States government. Neither the United States government nor any agency thereof, nor any of their employees, makes any warranty, express or implied, or assumes any legal liability or responsibility for the accuracy, completeness, or usefulness of any information, apparatus, product, or process disclosed, or represents that its use would not infringe privately owned rights. Reference herein to any specific commercial product, process, or service by trade name, trademark, manufacturer, or otherwise does not necessarily constitute or imply its endorsement, recommendation, or favoring by the United States government or any agency thereof. The views and opinions of authors expressed herein do not necessarily state or reflect those of the United States government or any agency thereof.

This report is available at no cost from the National Renewable Energy Laboratory (NREL) at www.nrel.gov/publications.

Available electronically at <http://www.osti.gov/bridge>

Available for a processing fee to U.S. Department of Energy and its contractors, in paper, from:

U.S. Department of Energy
Office of Scientific and Technical Information
P.O. Box 62
Oak Ridge, TN 37831-0062
phone: 865.576.8401
fax: 865.576.5728
email: <mailto:reports@adonis.osti.gov>

Available for sale to the public, in paper, from:

U.S. Department of Commerce
National Technical Information Service
5285 Port Royal Road
Springfield, VA 22161
phone: 800.553.6847
fax: 703.605.6900
email: orders@ntis.fedworld.gov
online ordering: <http://www.ntis.gov/help/ordermethods.aspx>

Cover Photos: (left to right) photo by Pat Corkery, NREL 16416, photo from SunEdison, NREL 17423, photo by Pat Corkery, NREL 16560, photo by Dennis Schroeder, NREL 17613, photo by Dean Armstrong, NREL 17436, photo by Pat Corkery, NREL 17721.



Printed on paper containing at least 50% wastepaper, including 10% post consumer waste.

Executive Summary

Power hardware-in-the-loop (PHIL) simulation testing of a 500 kW Satcon photovoltaic (PV) inverter was conducted at the Center for Advanced Power Systems (CAPS) at Florida State University (FSU) from March 12th through March 16th 2012. Testing was led by a team from the National Renewable Energy Laboratory (NREL). This report reviews the results of data captured during the course of testing. The tests were used to demonstrate operation of and gather data from the inverter in a simulated operational environment. In particular, testing demonstrated the ability of the inverter to operate in either a Power Factor Control Mode (constant power factor), or a Reactive Power Command Mode (constant reactive power), and to respond to real power limits.

The unit under test (UUT) was a Satcon 500 kW PowerGate Plus inverter with a native output voltage of 200 V. The inverter was connected to a variable DC signal from a variable voltage source (VVS) on the DC side, and a medium voltage (MV) transformer (200 V secondary/12.6 kV primary) connected to an AC VVS on the AC side. The DC VVS was programmed to follow a current reference which simulated one of two 15 minute irradiance scenarios. The AC VVS was configured to emulate an AC grid interconnection. Throughout testing, the system emulator measured and logged critical data at key test nodes with a time resolution of one second. In addition, high speed (0.065 to 1 msec) data was captured for certain test cases.

During the course of testing, five different parameters were varied:

- 1. Irradiance Profile:** Moderate or High
- 2. Inverter Location on the Distribution Feeder:** “Bus 3” (closer to the substation) and “Bus 31” (further from the substation)
- 3. Inverter Control Mode:** Constant Power Factor Mode or Reactive Power Command Mode¹
- 4. Inverter Command:** Depending on whether the inverter’s control mode was set to Constant Power Factor Mode or Reactive Power Command Mode, the inverter was provided with either a power factor command (1.0, 0.95, 0.9, 0.85, inductive), or a constant reactive power command (0 kVAr, 150 kVAr, or 300 kVAr, inductive).
- 5. Size of the Emulated PV Installation:** Simulations were conducted for both the “true” size of the emulated PV (500 kW), and for a scaled 2 MW installation. The 2 MW simulations scaled the inverter’s actual current and voltage output to simulate the effect of a larger plant on the local distribution system.

Analysis of the test results indicates that the test configuration appears to replicate real-world operation of a PV inverter, and that the tests successfully demonstrated operation of the inverter across a range of constant power factor commands, and a range of constant reactive power commands. Several issues surrounding the system’s response to limit conditions were identified for further investigation.

¹ Inverter outputs constant reactive power, up to the inverter’s rated capacity

The PHIL test configuration appears to closely replicate real-world operation of a PV inverter: Under a baseline configuration in which the inverter's power factor (PF) was set to 1.0, the inverter's power output was shown to closely track the reference signal. Minor fluctuations in the inverter's DC input were shown to be consistent with operation of the inverter's MPPT algorithm and the V-I profile assumed for the emulated PV installation. Occasional transient errors in the inverter's DC input signal under high power operation were attributed to a delay in the DC variable voltage source (VVS) which caused the inverter's MPPT to drift into a low-power regime.

The inverter's measured efficiency during testing tracks the inverter's rated CEC efficiency curve over its full range of power output. The measured efficiency was found to be systematically lower than the predicted efficiency by approximately 0.5% across the measured data points. We have speculated that this discrepancy is due to an unaccounted-for parasitic loss in the AC power measurement.

Demonstration of Power Factor Control Mode: The inverter was operated across a range of power factors from 0.85 to 1.0, inductive, over two different irradiance profiles. Consistent with expectations, the inverter's actual PF was shown to closely track the commanded power factor. The error in the inverter's measured PF was typically well below 1% of its steady state value. Two minor issues were noted during testing, both of which we believe are artifacts of the test configuration:

- The inverter's actual PF shows a systematic error of approximately 1% compared to the commanded PF. This result would be consistent with an unaccounted for measurement error in the AC power output.
- Rapid changes in the system's real power output tend to correlate with errors of up to 3% in the inverter's actual PF. We have speculated that the protection elements on the inverter's DC bus, by limiting the inverter's ability to rapidly circulate power, slow its ability to rapidly change the reactive power output.

Demonstration of Reactive Power Command Mode: In Reactive Power Command Mode, the inverter was operated with constant reactive power commands of -150 and -300 kVAR over two different irradiance profiles. During these tests, the inverter's real power limit was configured such that the inverter would always have sufficient capacity to meet the reactive command. Analysis of the results showed that the inverter's reactive power output was within 2% of the commanded level when the inverter remained below its kVA limit. As the inverter approached its kVA limit, this error increased to 5%-10%. Measurements of the AC voltage at the inverter's terminals and the point of interconnect showed that the generation of reactive power has a measurable impact on the voltage of the distribution feeder in question, and that this effect is significantly larger for increasing plant size.

Oscillations in real and reactive power output when operating near the inverter's power limit: When operating near its power limits, the inverter exhibited oscillations in its real and reactive power output. Investigation of the available data suggests that the oscillations may be attributable to a lag in the inverter's curtailment of reactive power under limit conditions which was exacerbated by the effect of reactive power on the voltage at the inverter's terminals. It is not

currently clear what caused the lag in the inverter's response or why the voltage at the inverter terminals showed such wide swings. These issues will be investigated in further tests.

Recommendations and Next Steps:

1. **PHIL Test Configuration:** The PHIL test environment offers a valuable tool to test inverter functionality in a controlled and flexible setting. To help facilitate data analysis, we would recommend that future PHIL tests include additional high speed data captures to help provide additional data as to the inverter's operating regime, and to help calibrate the data collection apparatus. The protection elements that were included in the test configuration may have had a minor impact on the test results, but are a critical element that should likely be included for future tests. We would recommend reviewing and monitoring the configurable voltage, current, and power limits to ensure that they are appropriate.
2. **Inverter Power Control Functions:** The inverter's Power Factor Control and Reactive Power Command Modes both function largely as expected. However, the observed oscillations in the inverter's real/reactive power output bear further investigation into the inverter controller's response under the specified conditions, as well as continued consideration of a yet-to-be-identified interaction with the test environment.

Abbreviations

AC	Alternating current
CAPS	Center for Advanced Power Systems
DC	Direct current
FSU	Florida State University
kVA	kilovolt ampere
kW	Kilowatt
MPPT	Maximum Power Point Tracking
MV	Medium voltage
MW	Megawatt
NREL	National Renewable Energy Laboratory
P	Real power
PF	Power Factor
PHIL	Power Hardware-in-Loop
Pu	per unit scaling between 0 and 1
PV	Photovoltaic
Q	Reactive power
S	Total real + reactive power, calculated as $\sqrt{P^2+Q^2}$
UUT	Unit under test
VAr	Volt-ampere reactive
VVS	Variable voltage source

Table of Contents

Executive Summary	iii
Abbreviations	vi
List of Figures	viii
1 Introduction	1
2 Approach	1
2.1 Test Configuration	1
2.2 Test Plan	3
3 Results and Analysis	4
3.1 DC-to-AC Power Conversion	4
3.1.1 Overview	4
3.1.2 Background on Maximum Power Point Tracking	4
3.1.3 Power Tracking and Power Conversion	6
3.1.4 Power Conversion Efficiency	11
3.1.5 Summary	11
3.2 Power Factor Control Mode	12
3.2.1 Overview	12
3.2.2 Test Results	12
3.3 Reactive Power Command Mode	18
3.3.1 Overview	18
3.3.2 Test Results	18
3.4 Effect of Reactive Power on Grid Voltage	22
3.5 Oscillations in Reactive Power Command Mode	23
4 Conclusions	29
5 References	31

List of Figures

Figure 1: Test configuration.....	2
Figure 2: Panel-level V-I characteristic at 1 pu	2
Figure 3: Sample reference irradiance signal and associated V/I operating points	6
Figure 4: Irradiance signal to DC Power to AC Power Transfer, Moderate Variability Scenario, PF=1.0	7
Figure 5: Irradiance signal to DC power to AC power transfer, high variability scenario, PF=1.0	7
Figure 6: Zoomed-in capture from t=400 to t=600 of high variability irradiance scenario, PF = 1.0 ..	9
Figure 7: Error between DC reference relative to the irradiance input	9
Figure 8: Inverter operating points, moderate variability (top) and high variability (bottom)	10
Figure 9: Measured efficiency vs. inverter's rated efficiency as a function of power output, PF=1.011	
Figure 10: Power factor control power limits.....	12
Figure 11: Inverter real vs. reactive power as a function of power factor, moderate (top) and high (bottom) variability scenario	13
Figure 12: Inverter power output as a function of power factor for moderate (top) and high (bottom) variability scenarios	14
Figure 13: Actual vs. commanded power factor as a function of time, high variability scenario	15
Figure 14: Actual vs. commanded power factor as a function of time, high variability scenario	16
Figure 15: PF error vs. time (top), and AC power vs. time (bottom).....	17
Figure 16: Illustration of Reactive Power Command Mode power limits	18
Figure 17: Inverter real and reactive power output in Reactive Power Command Mode, high variability (top) and moderate variability (bottom) irradiance scenarios	20
Figure 18: Inverter real vs. reactive power	21
Figure 19: Voltage at the inverter terminals (top) and voltage at the simulated point of interconnect (bottom). Left hand plots show plant size of 0.5 MVA, right hand plots show simulated plant size of 2MVA.....	22
Figure 20: Oscillations in Real and Reactive Power at the inverter's power limit	24
Figure 21: High-speed data capture for RTDS supplementary tests 1 and 2	25
Figure 22: High speed data capture of inverter AC voltage, AC Current, DC Voltage, and Real and Reactive Power (RTDS sup capture #1 and 2).....	25
Figure 23: High-speed data capture of inverter AC voltage, AC current, and DC voltage, PHIL in open loop configuration (RTDS sup capture #3).....	26
Figure 24: Comparison of inverter terminal voltage	27

1 Introduction

This test report analyzes the results of power hardware-in-the-loop (PHIL) simulation testing of a 500 kW Satcon photovoltaic (PV) inverter. The tests were conducted at the Center for Advanced Power Systems (CAPS) at Florida State University (FSU) from March 12th through March 16th, 2012. It complements the test report issued by FSU, which details the test procedure and overall test results [1]. This report presents independent analysis conducted by Satcon of data captured during testing. It will focus specifically on the operation of the inverter during testing. The purpose of the report is to present analysis that:

1. Validates the microgrid test configuration by verifying that the inverter responds to the environment in a manner that is consistent with an equivalent real-world application
2. Demonstrates two different power control modes of the inverter
3. Identifies areas for further development or refinement of the inverter's existing power control functions, and identifies potential issues or modifications to the PHIL test approach for future similar PHIL tests.

2 Approach

2.1 Test Configuration

A diagram of the test setup, reproduced from the FSU test report [1], is shown in Figure 1. The unit under test (UUT) was a Satcon 500 kW PowerGate Plus inverter with a native output voltage of 200 V. As shown, the inverter was connected to a variable DC signal from a VVS on the DC side, and a medium voltage (MV) transformer (200 V secondary/12.6 kV primary) connected to an AC VVS on the AC side. A more detailed description of the test set up is included in the FSU/CAPS test report.

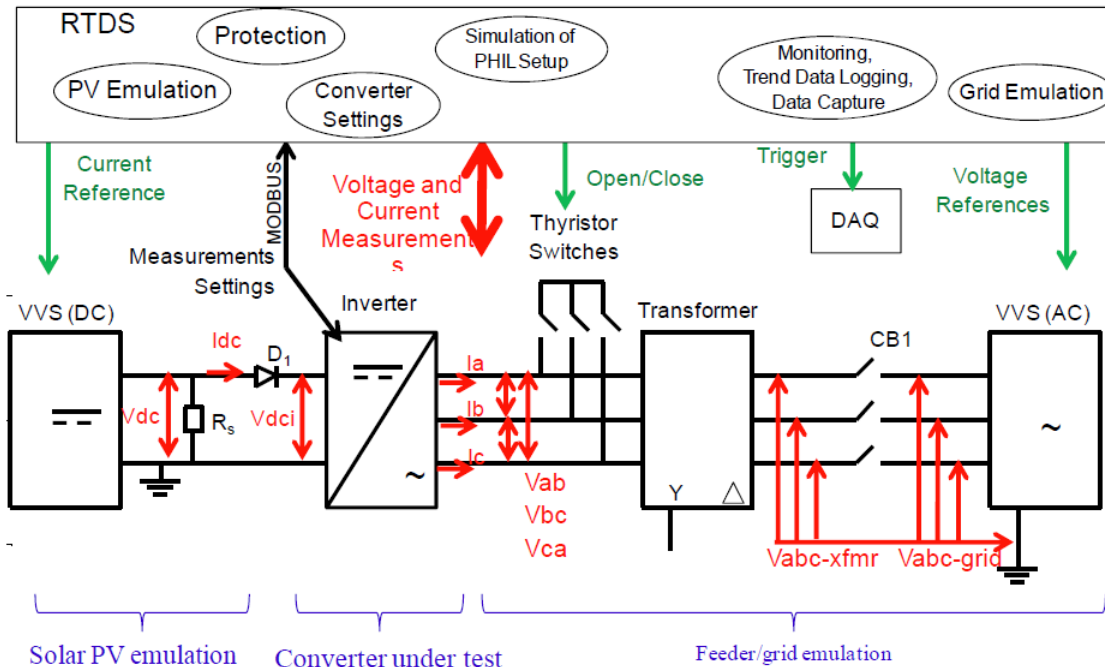


Figure 1: Test configuration

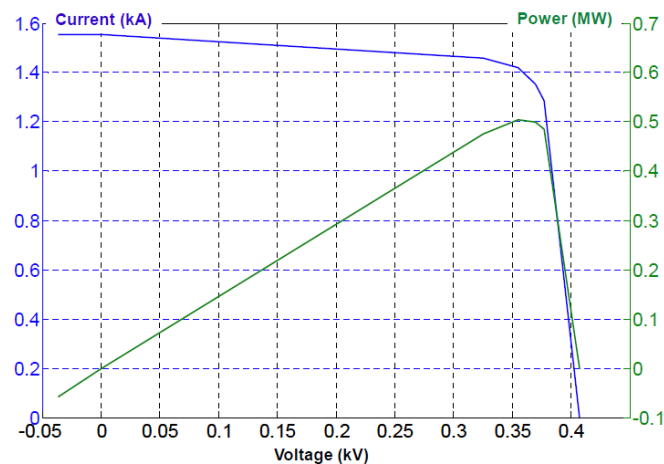


Figure 2: Panel-level V-I characteristic at 1 pu

The DC VVS was programmed to follow a current reference which simulated one of two 15 minute irradiance scenarios (a moderate variability and a high variability scenario). At a given point in time, the VVS output current was calculated a function of the input irradiance current reference, which was used to scale a pre-programmed V-I characteristic (Figure 2) between 0 (no power) and 1 (rated power); and the DC voltage, which was varied by the inverter according to its internal maximum power point tracking (MPPT) algorithm.

The AC VVS was configured to emulate an AC grid interconnection. It was configured to operate by sensing and adjusting the grid voltage and impedance seen by the inverter in response to pre-programmed distribution feeder models, and to the actual voltage and current output from the inverter.

The test configuration included several non-standard elements to provide an added layer of protection to the inverter and other test equipment. These non-standard elements included:

1. A DC load bank (~2.5 ohm) connected between the DC high and low voltage to provide damping
2. A series connected diode on the positive side of the DC connection to prevent back-feeding of power into the VVS
3. In addition, the PHIL controls included current, voltage, and rate limits to ensure that the test equipment remained within its nominal operating condition.

Broadly speaking, we do not believe that these protection elements materially affected the overall results of the inverter testing. However, these elements may in some cases have slowed the inverter's transient response or introduce unexpected power or current limits, which could have caused anomalous measurements. These issues are discussed in greater detail in Section 3.

Throughout testing, the system emulator measured and logged critical data at key test nodes. This data included time, the 3-phase AC primary, 3-phase AC secondary, and DC current and voltage; the input irradiance reference; real and reactive power; and emulated voltage at different buses along the emulated distribution feeder. Data was primarily logged at one second intervals, although a few high speed data captures of specific events were also gathered.

2.2 Test Plan

Prior to testing, a test plan was jointly developed by NREL, FSU CAPS, Quanta Technology, and Satcon Technology. Testing entailed initial commissioning tests of the PHIL closed loop AC voltage control, followed by a series of tests which operated the inverter in multiple operating modes in the emulated microgrid environment. For the emulated microgrid testing, inverter operation was tested while varying five different characteristics of the simulated environment:

1. **Irradiance Profile:** Moderate or High
2. **Inverter Location on the Distribution Feeder:** Bus 3 (closer to the substation) and Bus 31 (further from the substation)
3. **Inverter Control Mode:** Constant Power Factor Mode or Reactive Power Command Mode²
4. **Inverter Command:** Depending on whether the inverter's control mode was set to Constant Power Factor Mode or Reactive Power Command Mode, the inverter was provided with either a power factor command (1.0, 0.95, 0.9, 0.85, inductive), or a constant reactive power command (0 kVAr, 150 kVAr, or 300 kVAr, inductive).
5. **Size of the Emulated PV Installation:** Simulations were conducted for both the "true" size of the emulated PV (500 kW), and for a scaled 2 MW installation. The 2 MW simulations scaled the inverter's actual current and voltage output to simulate the effect of a larger plant on the local distribution system.

² Inverter outputs constant reactive power, up to the inverter's rated capacity

3 Results and Analysis

Subsequent to testing, data logs from the PHIL testing of the inverter were analyzed to evaluate system functionality and behavior. Satcon analyzed this data specifically to characterize and evaluate the inverter's operation. As such, we focused our analysis on measurements at the virtual PV site (i.e., the inverter's DC link, the inverter terminals, and the point of interconnect).

Data was captured at one second intervals for each of the two 15 minute irradiance scenarios. In addition, a limited amount of high speed data (one data set at 65 usec, one data set at 1 msec resolution) was captured to provide additional insight into some test results which appeared anomalous. The bulk of the below analysis focuses on the 1-second resolution data, which in general is useful for characterizing overall power flow, but it cannot characterize transient behavior at the level of a single electrical cycle. In addition, it can be difficult to distinguish causation given the lack of resolution relative to the inverter's control loop.

We reviewed results for the moderate and high variability cases with the inverter operating in Reactive Power Command mode and in Power Factor Control Mode across a range of inverter power commands. Initial review suggested that inverter operation at both points of interconnect ("Bus 3" and "Bus 31") were substantively the same. As such, the analysis included below focuses on the system results from just one of the bus connections. Similarly, because we have focused primarily on the inverter's performance, we have only analyzed the results of the scaled (2MW) system in the context of the effect of plant size on the local grid voltage.

3.1 DC-to-AC Power Conversion

3.1.1 Overview

To verify that the inverter's test configuration appropriately replicates a real-world operational environment, we reviewed the results to verify that the inverter's core power transfer capability operates as expected. Although there is insufficient data to analyze the inverter's sub-second response, the data captures were used to verify that: (1) the inverter's maximum power point tracking (MPPT) algorithm and the DC VVS operate as expected; (2) the inverter's power output tracks the reference irradiance signal; and (3) the inverter's power conversion losses are consistent with the inverter's CEC efficiency ratings.

3.1.2 Background on Maximum Power Point Tracking

As a starting point for discussion, it is useful to provide some background information on the inverter's maximum power point tracking (MPPT) algorithm. The power output for a solar panel or collection of solar panels at a given irradiance condition is a function of the panels' operating voltage. A characteristic power curve for a panel (such as that shown in Figure 2) typically shows a linear increase in power as voltage increases and current remains constant up to its maximum power, at which point the panels' current sharply decreases as voltage increases.

The inverter's MPPT algorithm is designed to optimize power extraction from the array of connected PV panels. It does so by perturbing the DC voltage around its current operating point, sensing the result, and, based on whether the change in voltage increases or decreases power compared to the previous state, it again adjusts the DC voltage. Given these general operating parameters, one would therefore expect the MPPT algorithm employed on Satcon inverters to exhibit the following characteristics during operation:

1. During steady state operation (i.e., constant power output from the emulated PV array), the inverter's DC input should track the reference irradiance, but with some variance around the reference signal. For a data capture with 1-second resolution, such as those captured during the FSU testing, this variance will appear random, as it is considerably slower than the MPPT's control bandwidth.
2. In theory, the inverter could experience a sudden drop in power if the MPPT voltage gets on the "wrong" (high voltage) side of the knee in the MPP curve. Conversely, power output will remain relatively stable as long as the MPPT keeps the DC voltage on the left-hand side of the knee in the MPP curve, but would generally decrease with decreasing voltage.

An example data capture that helps illustrate operation of the inverter's MPPT algorithm is shown in Figure 3. The top figure shows the reference irradiance input, which is a series of constant power output commands ranging from 5% to 100% of the inverter's rated power. The bottom figure shows the inverter's actual DC voltage and current operating points throughout the data capture, overlaid with scaled V/I curves based on the pre-programmed V-I curve shown in Figure 2. As shown, the VVS appears to operate along the constant power lines as expected.

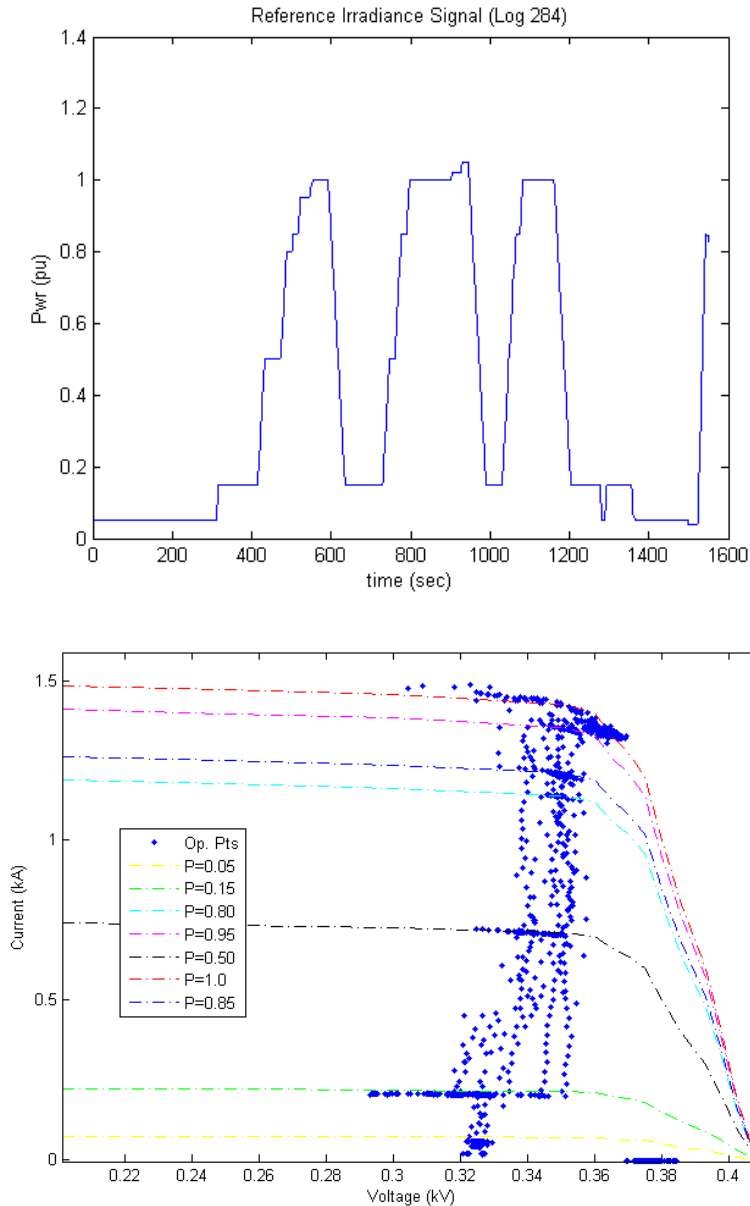


Figure 3: Sample reference irradiance signal and associated V/I operating points

3.1.3 Power Tracking and Power Conversion

Data captures of the PV reference signal, the VVS DC output, the inverter’s DC input, and the RMS AC output vs. time for the moderate and high variability profile are shown in Figure 4 and Figure 5, respectively. In both cases, the inverter is operated in Power Factor Command Mode, with the Power Factor set to 1. As shown, the DC VVS output to the inverter (black) generally tracks the PV reference signal (blue). In turn, the DC input to the inverter (red) tracks the VVS output minus losses due to the series connected diode and the resistive load bank included as protective elements. The AC voltage (green) closely tracks the inverter’s DC input, minus power conversion losses.

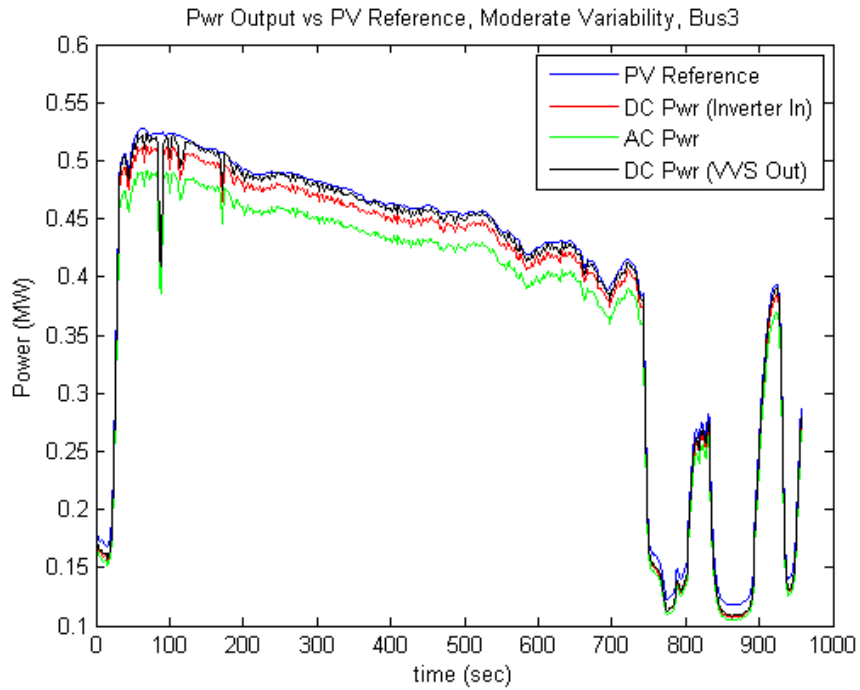


Figure 4: Irradiance signal to DC Power to AC Power Transfer, Moderate Variability Scenario, PF=1.0

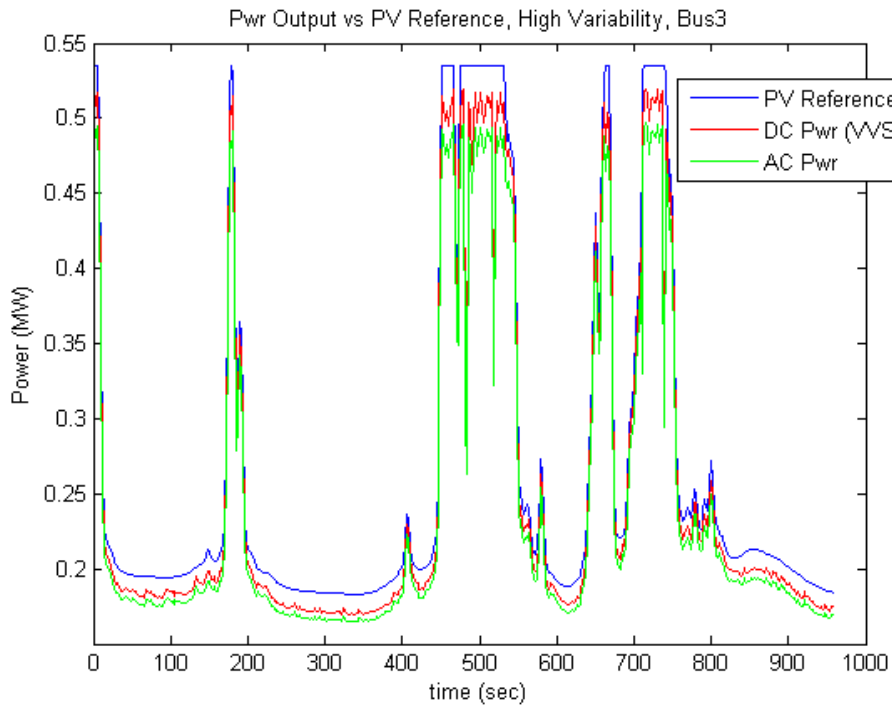


Figure 5: Irradiance signal to DC power to AC power transfer, high variability scenario, PF=1.0

The small variations around the DC reference (e.g., as visible from time = 300 to time = 600 sec in Figure 4) are consistent with operation of the inverter's MPPT algorithm. As discussed above, the inverter's MPPT algorithm operates by perturbing the DC link voltage to sense the optimal operating point given current irradiance conditions, so one would expect the DC signal to track the reference, but to include some high frequency perturbations, which are on the order of 1-2% of the inverter's power output.

Of greater interest are the occasional transient departures of the inverter's output from the reference signal. That is, while the inverter's DC link closely follows the PV reference at power levels below the inverter's 500 kVA power rating, when the reference power output exceeds the inverter's kVA rating, there are occasional transient excursions in which the error in the DC input signal to the inverter (i.e., the difference between the power reference and the actual power on the DC link) is significantly more pronounced. These deviations are most visible in Figure 5, or at $t < 200$ in Figure 4. For reference, a zoomed in capture of the high variability scenario from $t = 400$ to $t = 600$ is shown in Figure 6.

In general, the error in the VVS output (defined as the VVS DC power output divided by the reference input) is $< 10\%$, and at high power, well under 5% of the total (Figure 7). However, at power > 1 pu, there are occasional transients that are significantly larger (see $t = 500$ in Figure 5). Upon examination of the inverter's V-I operating points, it is apparent that these transient errors are due to the inverter's MPPT algorithm getting on the wrong side of the knee in the MPP curve. This behavior is illustrated in Figure 8, which shows the pathway of the V-I operating points for the moderate (top) and high (bottom) variability scenarios. In both data sets, the points corresponding to a DC power error $> 10\%$ are marked with a black circle. In virtually every case, these correspond to aberrantly high voltages, which in turn lead to low current.

While it is currently not clear why the MPPT algorithm allows the voltage to drift into this low power regime, after further discussions with FSU, we believe that these transients could be an artifact of the test configuration. During testing, the DC VVS's power limit settings were configured to use a filtered measurement for the DC voltage, but used an unfiltered measurement for the DC current. It appears that this caused the VVS to occasionally detect a power limit condition during periods of high irradiance when none was present, thereby limiting the VVS output current. Such a power limit condition would in effect introduce a mismatch between the response time of the VVS and the inverter's MPPT algorithm. In turn, the standard perturbation of the DC voltage would not register any change in current, which would cause the MPPT to move the voltage upward until the current was no longer limited.

It is also possible that the observed behavior reflects a miscalibration in the inverter's MPPT algorithm, which makes it over-aggressive when it nears the knee in the MPPT curve. However, the system only exhibits this behavior at the systems power limit, which would suggest that the cause is connected to a power limit in the inverter or the testing environment.

It should be noted that without a high speed data capture of this particular behavior, we cannot draw a firm conclusion as to the cause. However, this does suggest an area for additional examination during subsequent testing.

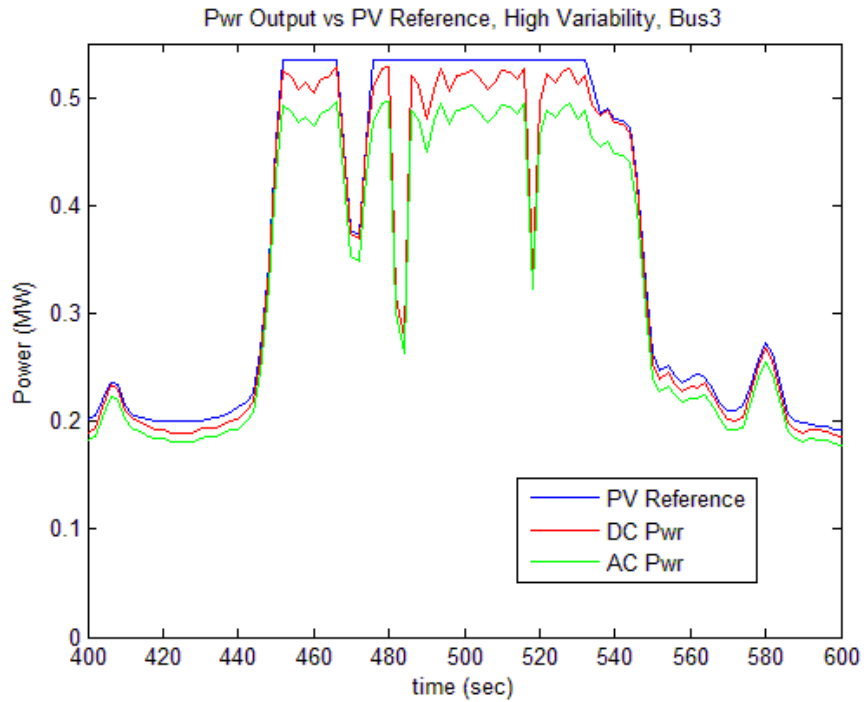


Figure 6: Zoomed-in capture from t=400 to t=600 of high variability irradiance scenario, PF = 1.0

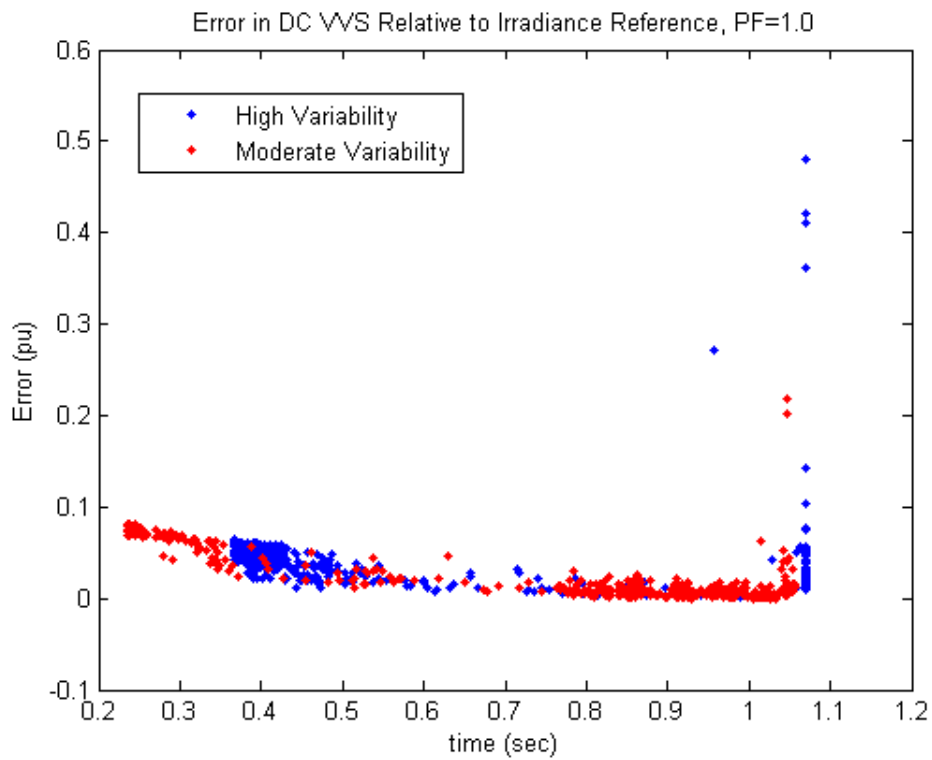


Figure 7: Error between DC reference relative to the irradiance input

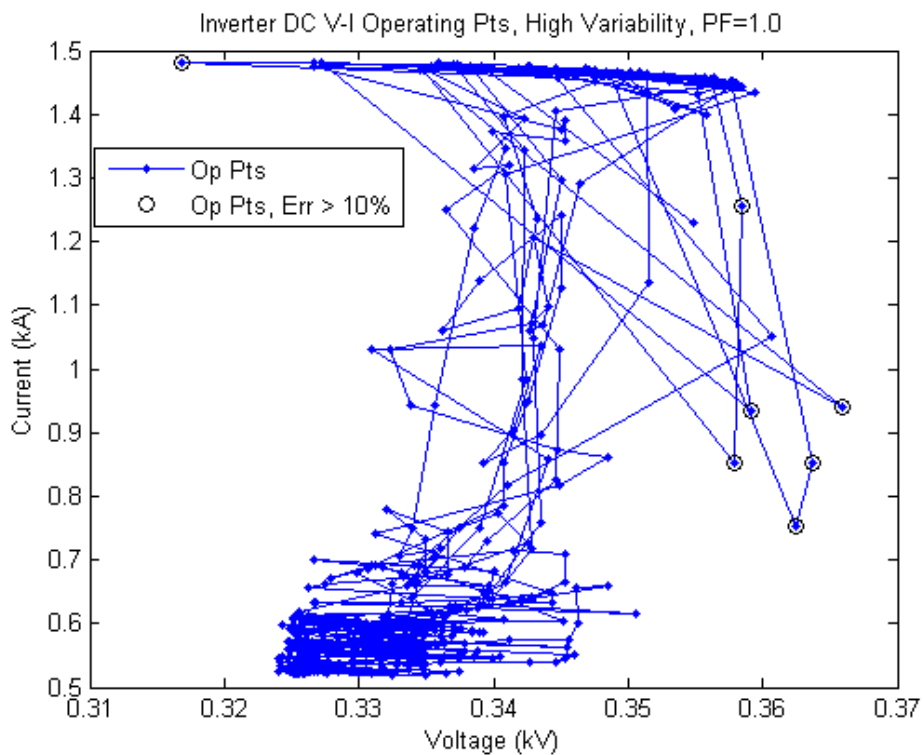
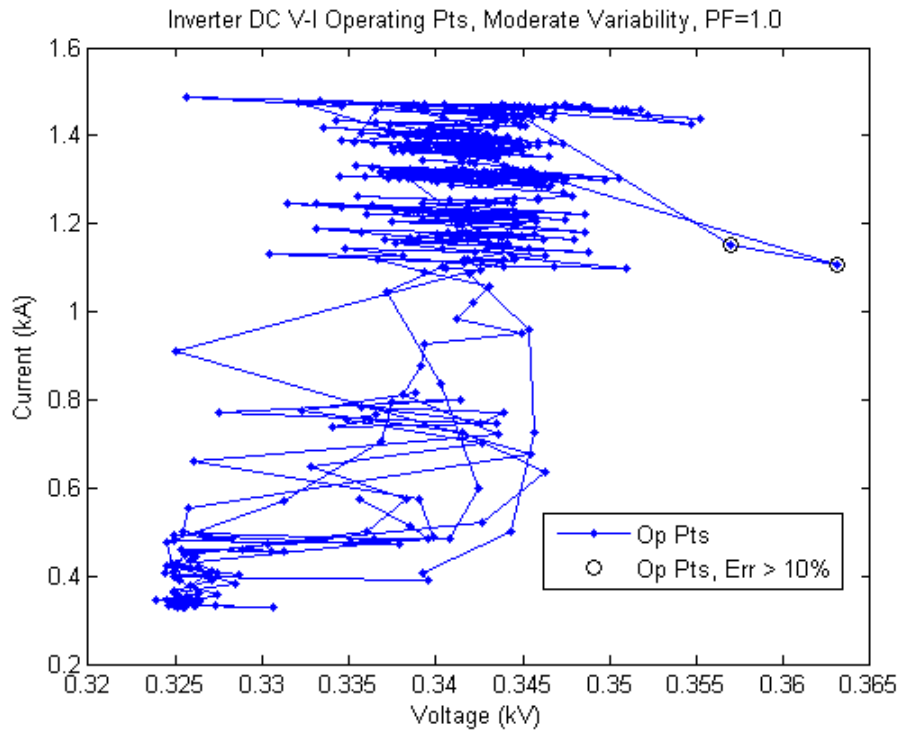


Figure 8: Inverter operating points, moderate variability (top) and high variability (bottom)

3.1.4 Power Conversion Efficiency

The inverter's power conversion efficiency, defined as the ratio of AC power to DC power is shown in Figure 9. For reference, the inverter's CEC operating efficiency³ at two different DC operating voltages is shown with dashed lines. In general, the DC voltage during testing ranged between 320 and 365V, so we would expect efficiency to nominally track between the two efficiency curves. The actual efficiency curve closely matches the predicted efficiency curve: the slope of the curves is nearly identical, while there appears to be a persistent error on the order of 0.5%. Such an error would be consistent with a systematic error in either the AC or DC power measurement, or some unaccounted for parasitic load.

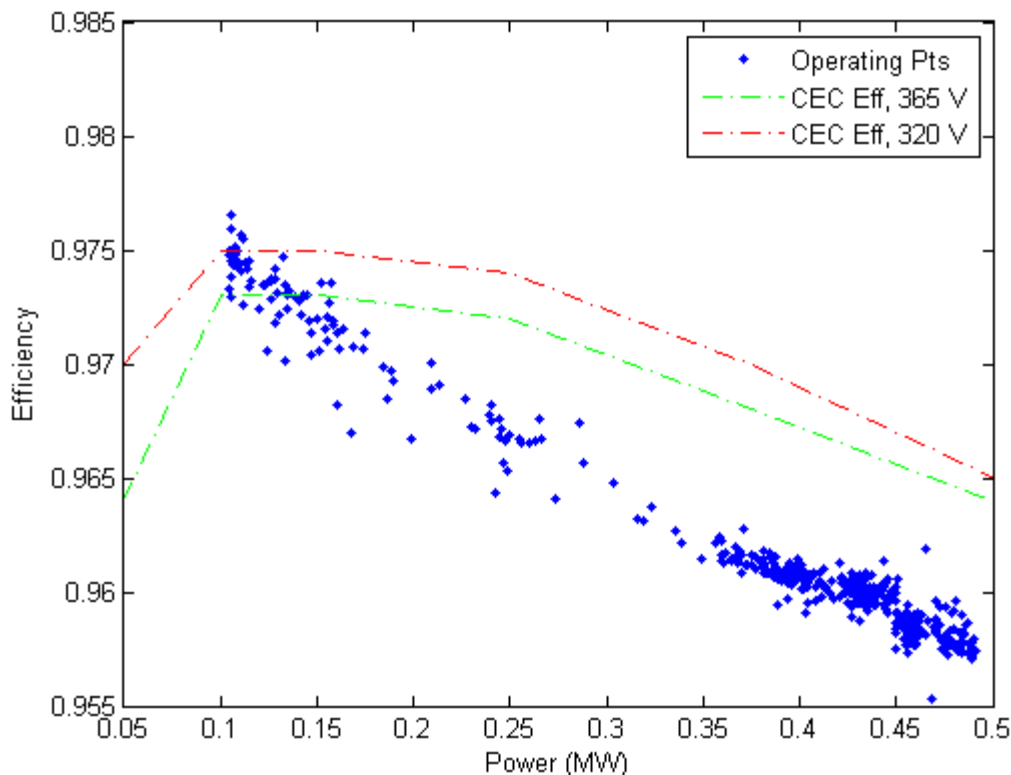


Figure 9: Measured efficiency vs. inverter's rated efficiency as a function of power output, PF=1.0

3.1.5 Summary

Analysis of basic DC-to-AC power conversion indicates that the inverter operates largely as expected within the microgrid test environment. In particular,

3. The inverter power output tracks the reference signal, and shows losses consistent with expectations.
4. In general, the VVS output current and the inverter's MPPT operate as expected. There is an open question around the DC voltage's tendency to periodically drift to the low power regime of the V-I curve when the inverter is operating at near its power limit. We have speculated that this is an artifact of how the VVS power limits were implemented in the test facility, but are unable to confirm without further testing.

³ http://www.gosolarcalifornia.org/equipment/inverter_tests/summaries/SatCon%20PVS-500%20%28MVT%29.pdf

3.2 Power Factor Control Mode

3.2.1 Overview

The inverter was operated in Power Factor Control Mode with PF settings of 0.85, 0.9, 0.95, and 1.0. In Power Factor Control mode, the inverter varies the reactive power output to maintain a constant (user-defined) power factor. The real and reactive power control limits for Power Factor Control Mode are shown in Figure 10. The PF may be commanded to any value between 0.8 and 1.0, leading or lagging. For $PF < 1$, the inverter's real power output is limited by the power factor command.

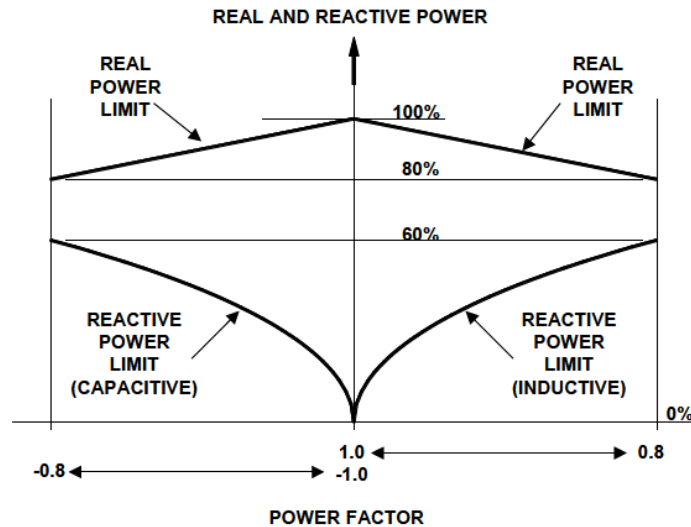


Figure 10: Power factor control power limits

3.2.2 Test Results

A plot (Figure 11) of the inverter's real vs. reactive power for the moderate (top) and high (bottom) variability scenarios illustrates the performance of the inverter's Power Factor Command mode. Each of the four sets of data points represents a different power factor command. As shown, at constant power factor, the real vs. reactive power curve is represented by a straight line projecting from the origin with a slope approximately equal to the commanded power factor. The line is bounded on one side by the origin (corresponding to zero power), and on the other side by a circle that corresponds to the inverter's power limit ($S = \sqrt{P^2 + Q^2}$). In power factor mode, this power limit has the effect of curtailing real power output during periods of high irradiance for $PF < 1.0$ (Figure 12).

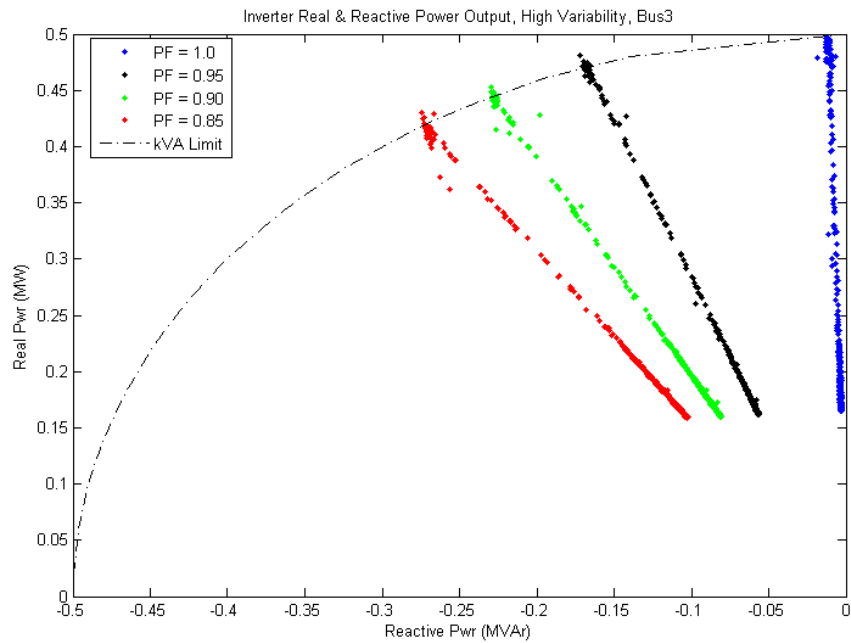
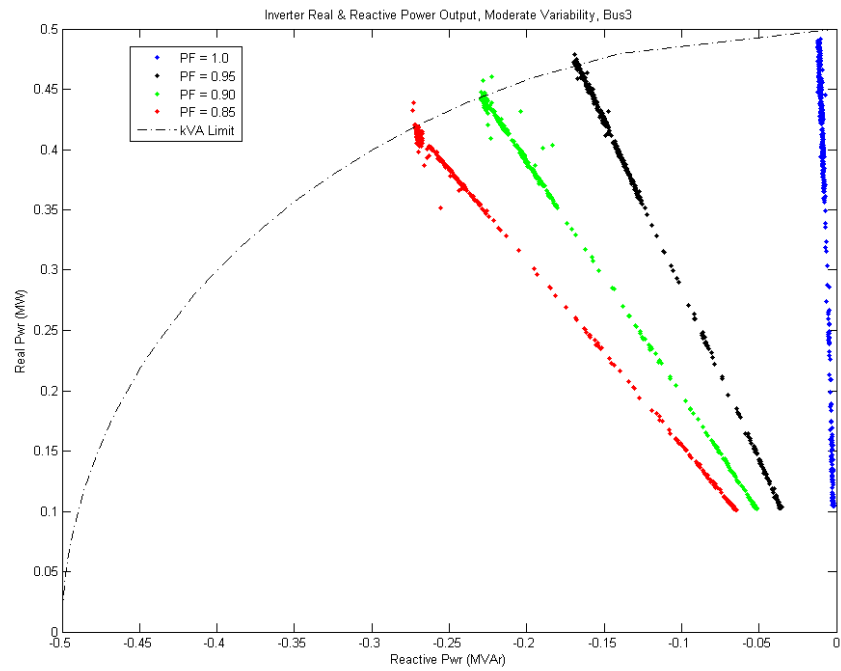


Figure 11: Inverter real vs. reactive power as a function of power factor, moderate (top) and high (bottom) variability scenario

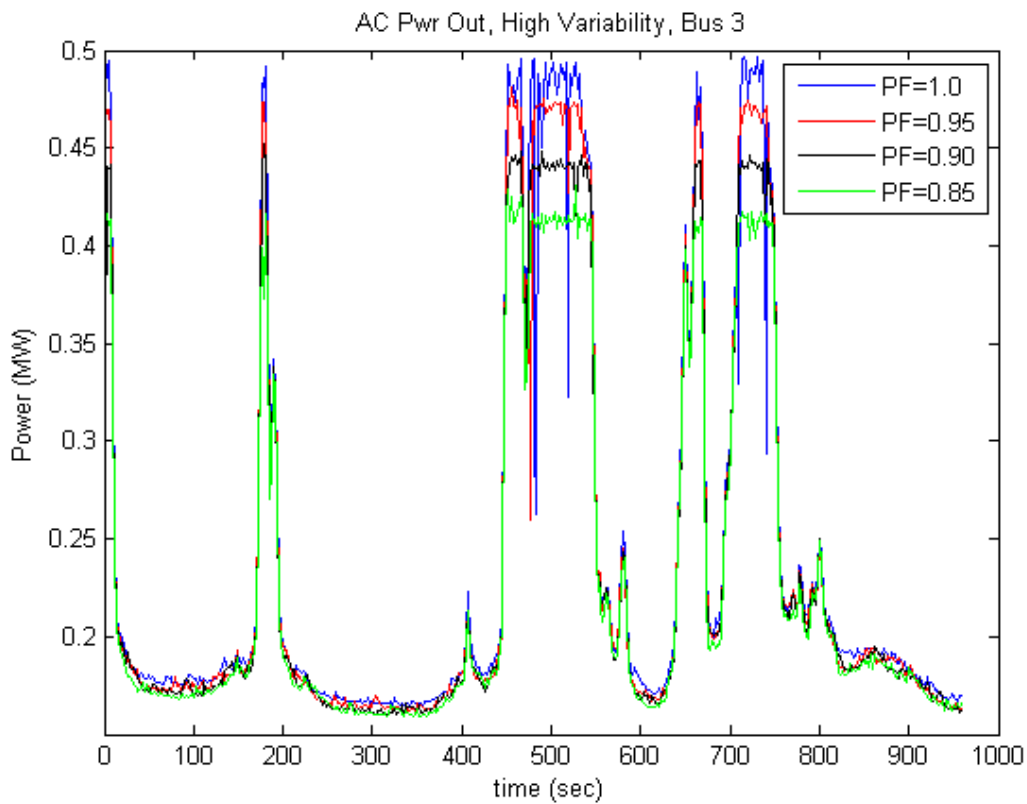
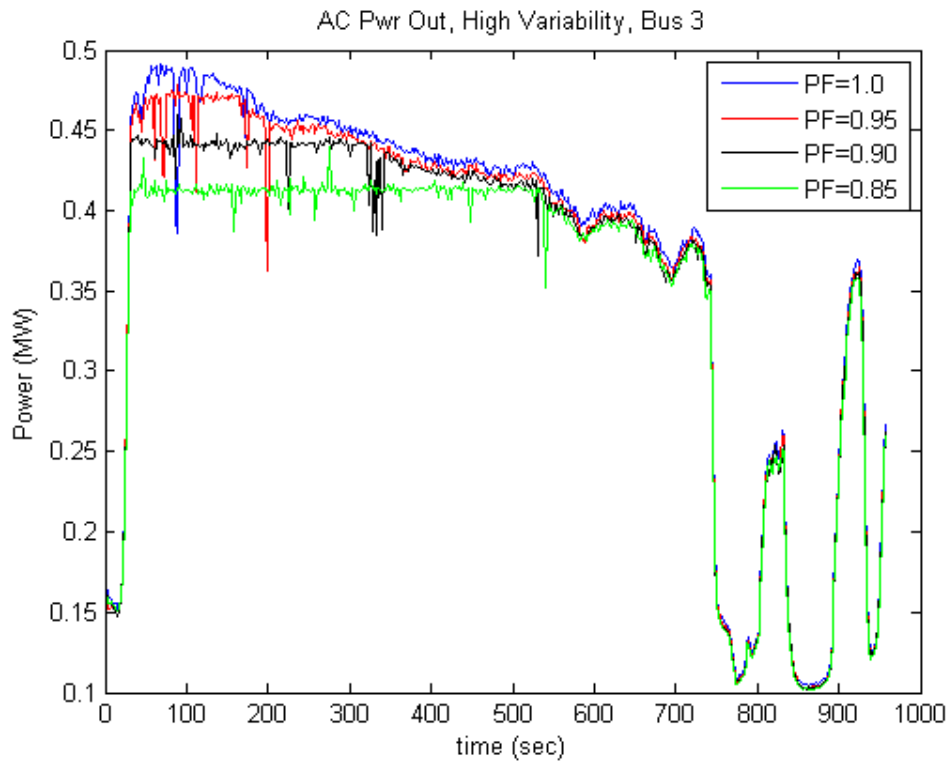


Figure 12: Inverter power output as a function of power factor for moderate (top) and high (bottom) variability scenarios

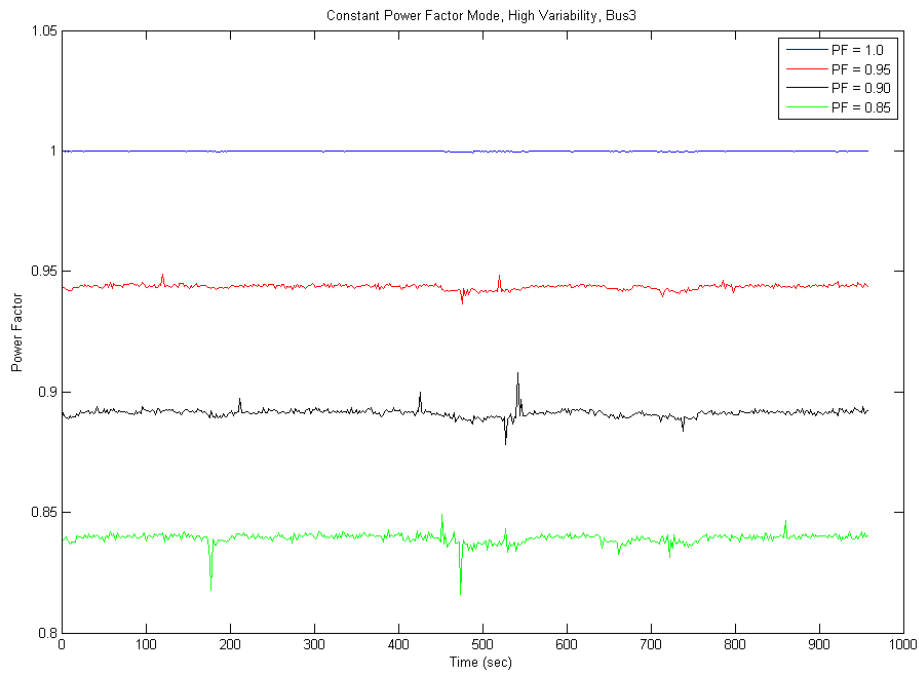


Figure 13: Actual vs. commanded power factor as a function of time, high variability scenario

When PF vs. time is examined for each of the irradiance scenarios, it is apparent that the system tracks the PF command (Figure 13).⁴ However, at $PF < 1.0$, there is a systematic error in which the actual PF is slightly lower than the commanded level (i.e., for PF command = 0.95, actual PF is approximately 0.94). Given that we observed a similar systematic error in the inverter’s power conversion efficiency calculation, we speculate that this reflects a measurement error at the PHIL facility. This question will be explored in subsequent testing, but does not reflect a significant cause for concern.

⁴ The results for the moderate variability scenario are substantively the same

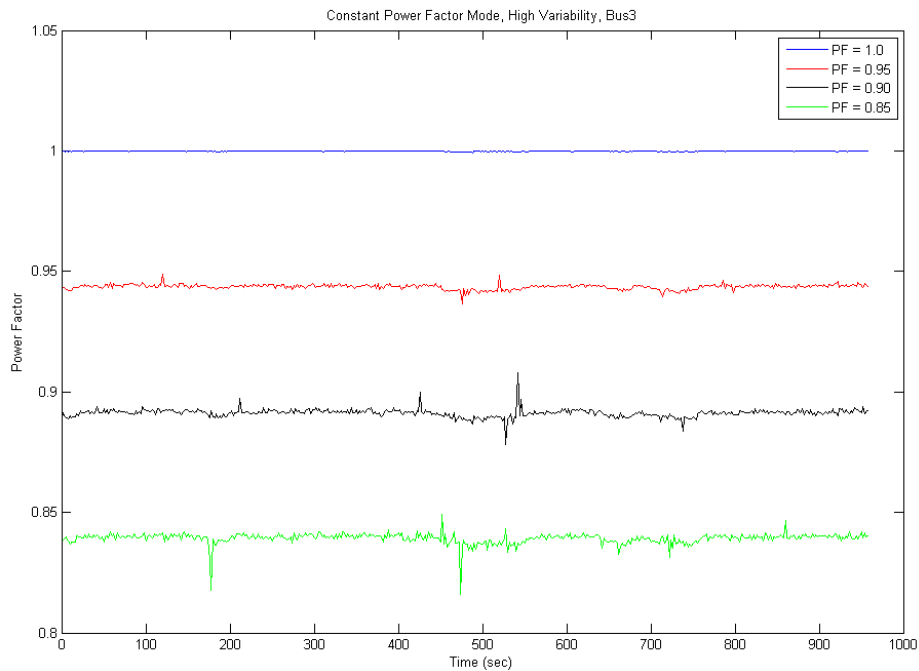


Figure 14: Actual vs. commanded power factor as a function of time, high variability scenario

A plot of the PF error (actual PF/commanded PF) vs. time is shown in Figure 14 (top). In addition to the above-noted systematic error, occasional transient deviations from the commanded power factor of approximately $\pm 3\%$ of the PF command are evident during rapid transients in the reference irradiance signal. For reference, the system's AC power output is shown in the bottom figure. For example, the two largest deviations (PF=0.85, in green at $t \sim 180$ sec, and $t \sim 480$ sec) correspond to rapid changes in the system's power output. We speculate that this relatively slow response of the inverter's reactive power output is due to the presence of the protective elements (load bank and diode) on the DC link, which slows the ability of the inverter to circulate/absorb reactive power.

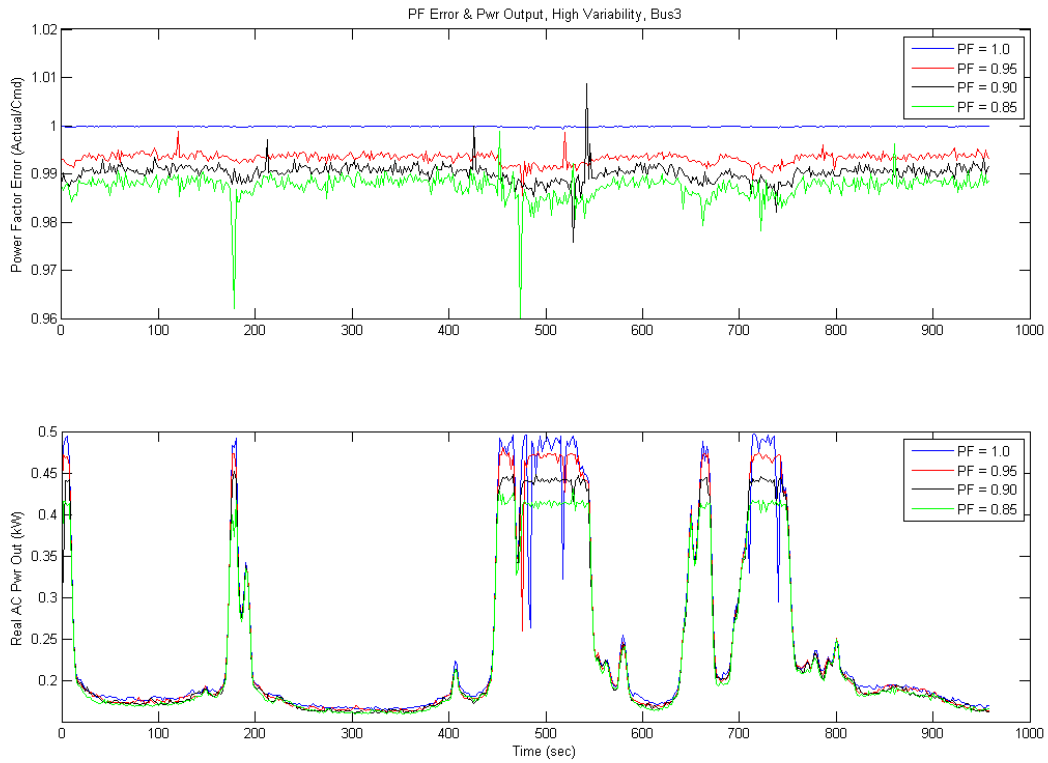


Figure 15: PF error vs. time (top), and AC power vs. time (bottom)

3.3 Reactive Power Command Mode

3.3.1 Overview

The inverter was operated in Reactive Power Command Mode with reactive power commands of 0 kVAr, -200 kVAr, and -300 kVAr. In Reactive Power Command Mode, the inverter outputs constant reactive power, up to the inverter's KVA rating. If the sum of the prevailing real power limit and the reactive power command exceed the inverter's power rating, the reactive power command is reduced to remain within the inverter's limits.

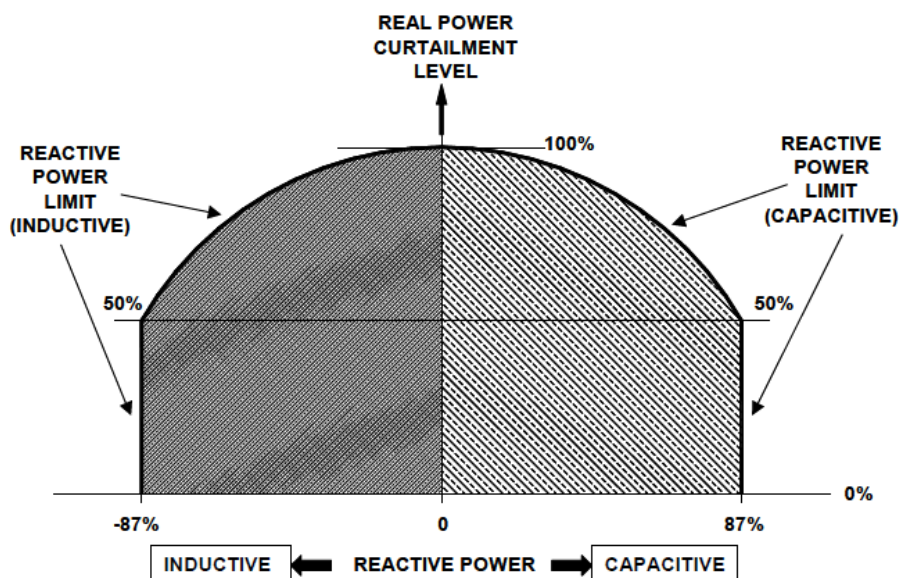


Figure 16: Illustration of Reactive Power Command Mode power limits

During initial testing of the reactive power mode, the inverter's real and reactive power were observed to oscillate when the inverter reached its 500 kW power rating, which suggested that the inverter was either adversely interacting with the FSU test environment, or that the inverter's regulator does not correctly handle the limit condition. These test results are discussed in greater detail below (Section 3.3.2).

To enable continued testing of the inverter's Reactive Power Command Mode, during subsequent testing, the inverter's real power limit was set such that the sum of the real power limit and reactive power command was slightly below the inverter's power rating. Limiting the real power output ensured that the inverter maintained constant reactive power output throughout the test scenarios.

3.3.2 Test Results

A plot of the inverter's real and reactive power output for the high (top) and moderate (bottom) variability scenarios is shown in Figure 16. As shown, the real power for the 150 kVAr case (red) is slightly curtailed due to a real power limit of 475 kW. For the 300 kVAr case (black), the inverter's real power limit is set to 400 kW. As such, the inverter's real power output is curtailed for significant periods of both scenarios (evidenced by the periods in which the power output "flat tops"). Figure 17 shows the inverter's real power output plotted against the reactive power

output throughout the data capture. The dashed line represents the inverter's kVA power limit for a given reactive power command. As shown, for each scenario, the inverter's reactive power output is nearly constant while the real power varies.

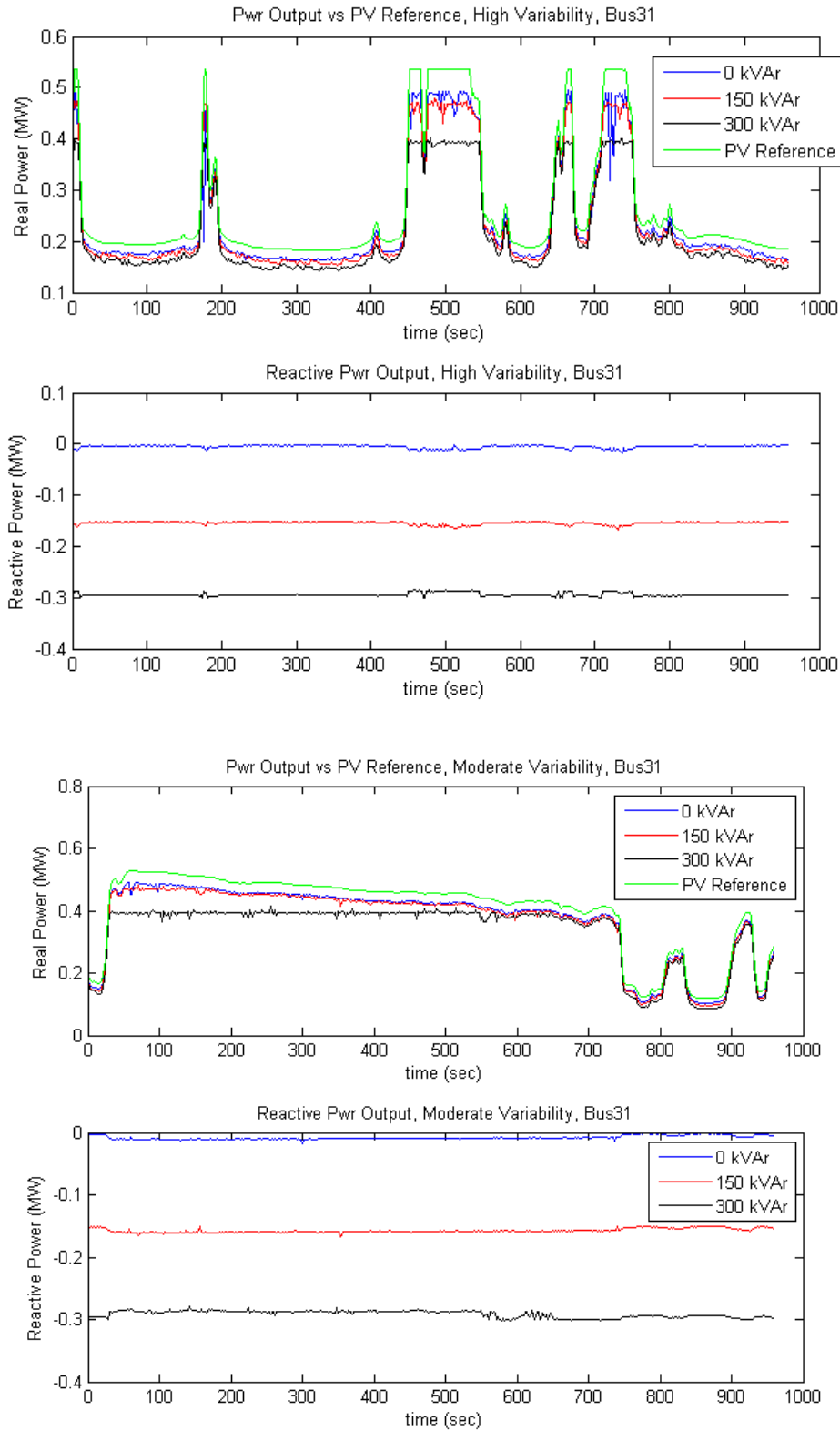


Figure 17: Inverter real and reactive power output in Reactive Power Command Mode, high variability (top) and moderate variability (bottom) irradiance scenarios

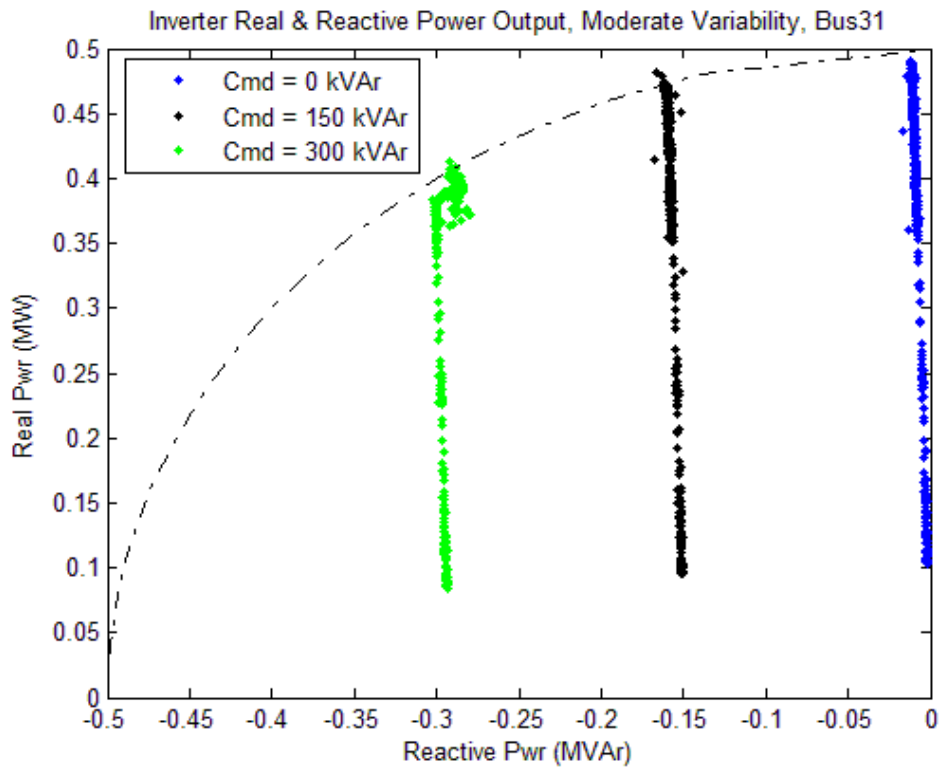
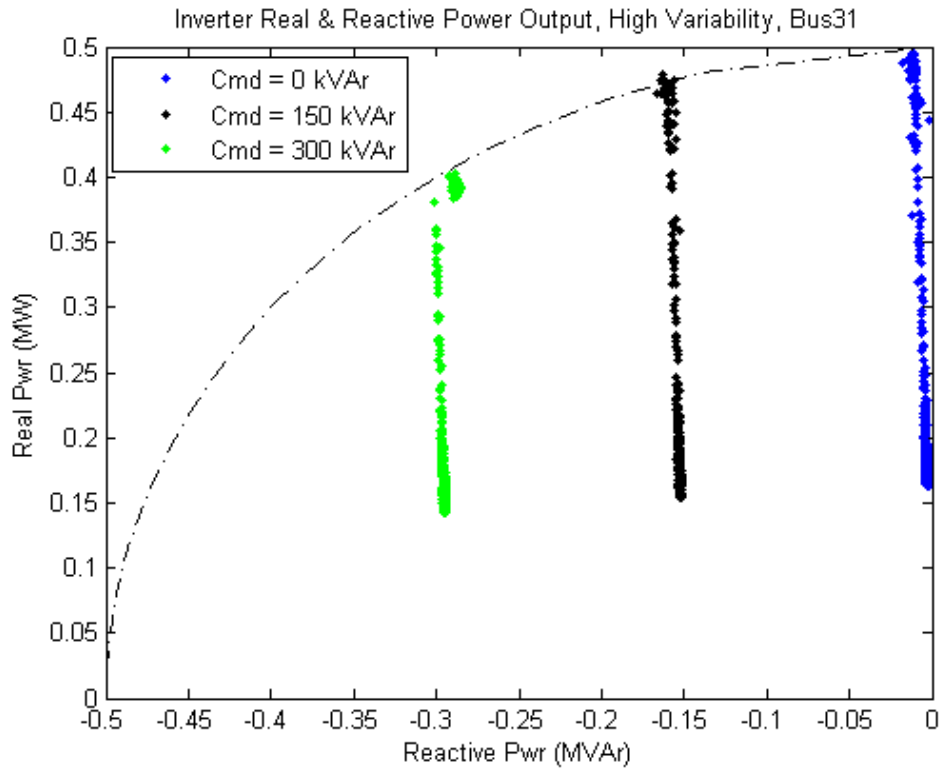


Figure 18: Inverter real vs. reactive power

3.4 Effect of Reactive Power on Grid Voltage

Although Satcon did not conduct independent testing or validation of the emulated distribution feeder, we reviewed the results to evaluate, in a qualitative sense, the effect of real and reactive power on the localized grid voltage. Testing showed that the inverter’s reactive power level had a measurable impact on the AC grid voltage at the point of interconnect.

During the course of testing, voltage was measured at the inverter’s terminals (transformer secondary, nominal voltage of 0.2 kV) and at the point of interconnect (transformer primary, nominal voltage of 12.6 kV). As shown in Figure 18 (top set of plots), injection of (inductive) reactive power causes the voltage at the inverter terminals (i.e., the transformer secondary) to go down by approximately 2% for the -150 kVAr case, and 4% for the -300 kVAr case, which is directionally consistent with what one would expect. These results are the same regardless of whether plant size is 0.5 MVA (left plot) or 2 MVA (right plot).

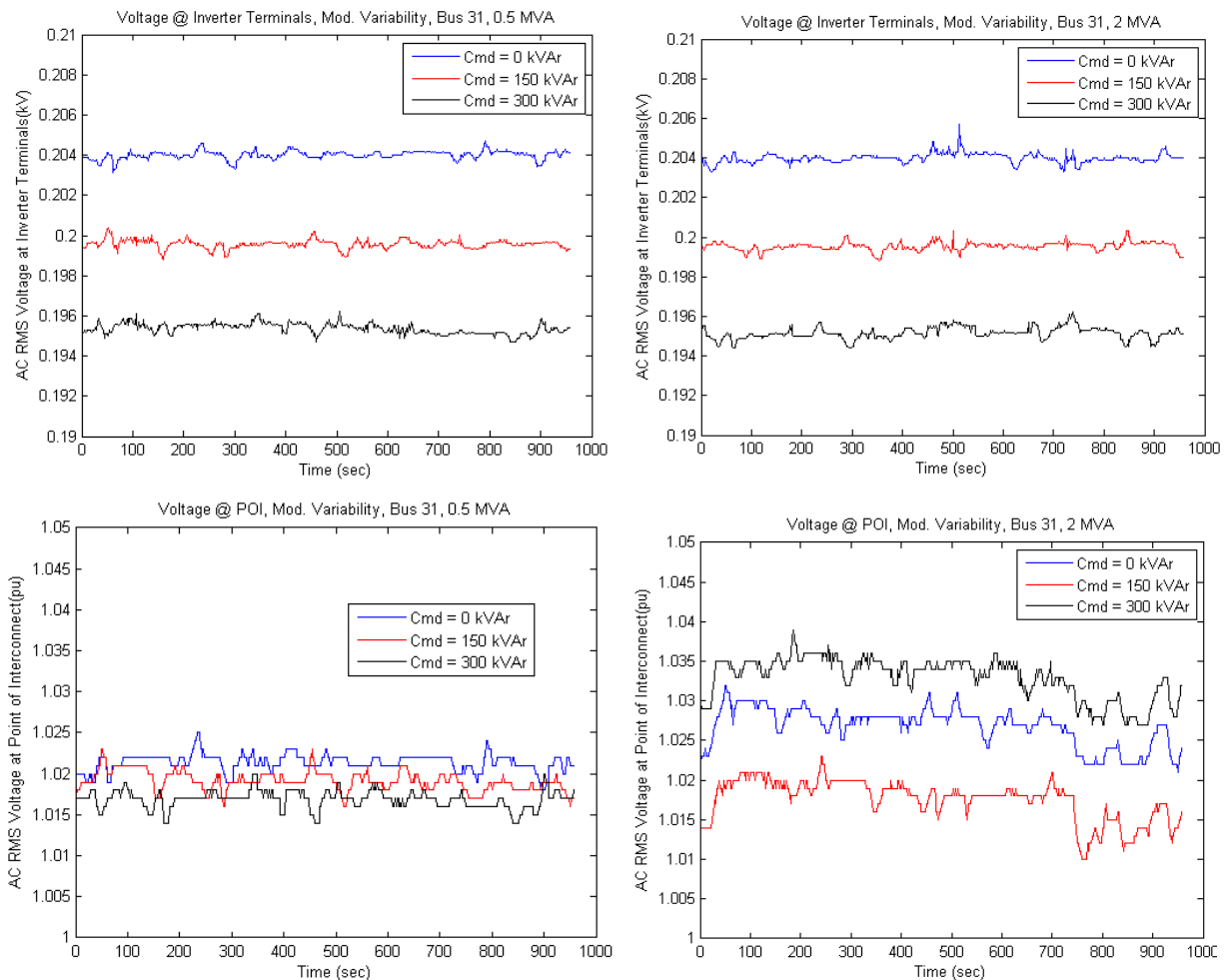


Figure 19: Voltage at the inverter terminals (top) and voltage at the simulated point of interconnect (bottom). Left hand plots show plant size of 0.5 MVA, right hand plots show simulated plant size of 2MVA.

The effect of reactive power on voltage is less pronounced, but still visible, when voltage is measured at the transformer primary (Figure 18, bottom set of plots), due to the impedance of the grid. For the 0.5 MVA case (left hand, bottom plot), the voltage on the feeder goes down by approximately 0.3% for each successive increase in reactive power. For the 2 MVA case (right hand plot), the effect of reactive power on the grid voltage is more pronounced, as the total power injection is considerably higher. For example, moving from 0 to -150kVAr moves the voltage down by approximately 1%. Note that for the 2 MVA tests, the -300 kVAr case results in higher voltage measured at the POI. This is due to a change in the capacitor bank configuration, which moves the local voltage set point upwards.

3.5 Oscillations in Reactive Power Command Mode

During the course of testing, oscillations in the inverter's real and reactive power output were noted when the inverter was operated in Reactive Power Command Mode. These oscillations were specifically noted under the following test conditions:

1. Configured in Reactive Power Command Mode
2. Reactive power command of -200 kVAr, but not -100 kVAr
3. The inverter's real power was not limited
4. The vector sum of the prevailing real power and the reactive power command exceed the inverter's kVA rating (i.e., $\sqrt{P^2+Q^2} > 1 \text{ pu}$)

In theory, for the above set of conditions, the inverter should reduce its reactive power to remain within the inverter's power limits, while delivering as much real power as available. However, it should be noted that, in practice, there is very limited operational experience with the inverter operating in these conditions. (i.e., for prior field deployments of the Reactive Power Command Mode, the reactive power command has been considerably lower, and the inverter has been configured to limit real power such that there is always capacity available to meet the reactive power command). When these oscillations were noted, the planned test procedure was modified to limit the inverter power, which was more consistent with prior operational experience.

Subsequent to testing, we reviewed data, the test configuration, and the inverter's control algorithms to try to identify a plausible mechanism for the observed behavior. A data capture of one of the tests in question is shown in Figure 19. As noted above, the reactive power command was -200 kVAr. As shown, the inverter's real and reactive power are stable and follow the reference command until the inverter approaches its kVA limit. At this point, both the real and reactive power begin varying considerably off of their respective set points. The variations in real power are on the order of 20% of the inverter's power reference (i.e., variation of 100 kW for a reference signal of roughly 500 kW). The variations in reactive power are also on the order of 100 kVA, but on a command of -200 kVA.

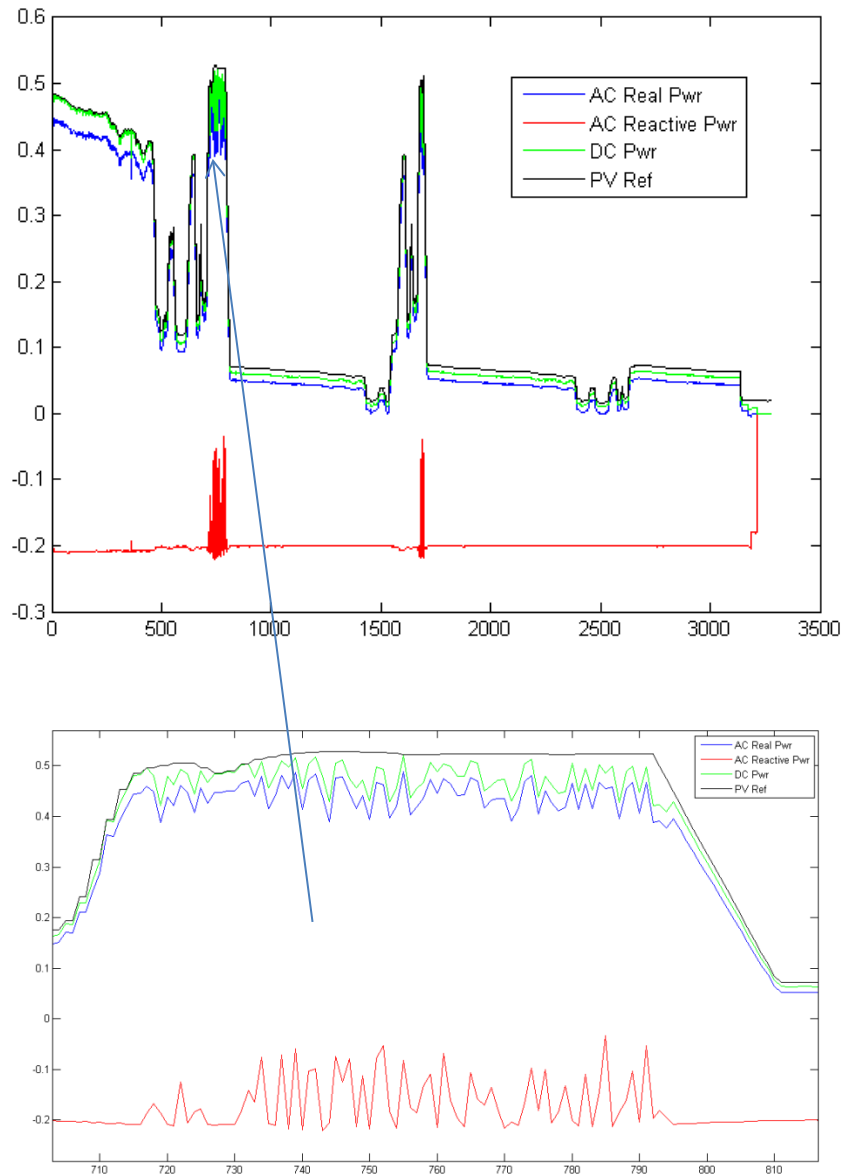


Figure 20: Oscillations in Real and Reactive Power at the inverter's power limit

In addition to the low resolution data, a brief high resolution capture (0.4 second duration, 65 usec resolution) of the test run in question was taken during testing (Figure 20). Figure 21 shows similar data, but scales several of the data points to a reference value of one pu (marked by the red dash line). It should be noted that some of the data represents filtered quantities (and hence is delayed), so it is somewhat difficult to distinguish the precise sequence of events. An additional high speed data capture (constant real power reference signal at > 1 pu, constant reactive power of -200 kVAr, 2 second duration, 1 msec resolution) in which the PHIL's closed loop voltage regulation was disabled shows similar oscillations (Figure 21). Unfortunately, we only have high speed data captures of anomalous behavior, so there is no baseline to compare against.

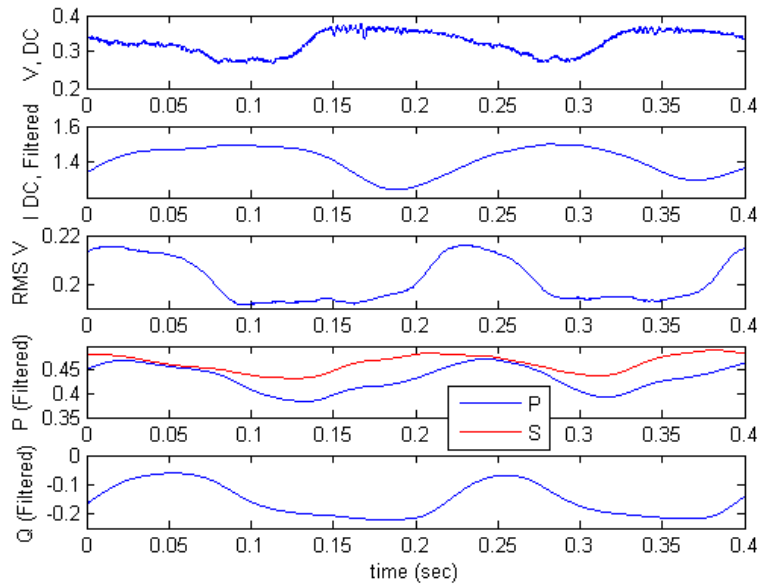


Figure 21: High-speed data capture for RTDS supplementary tests 1 and 2

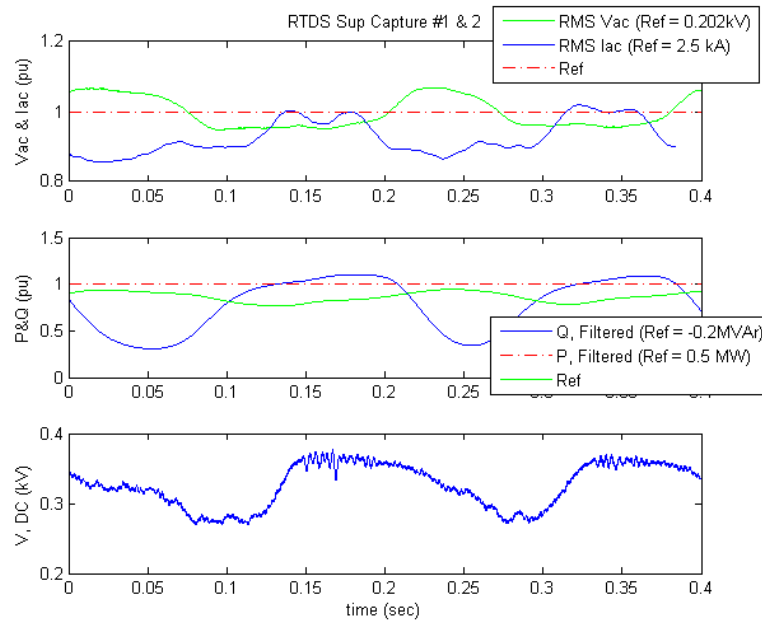


Figure 22: High speed data capture of inverter AC voltage, AC Current, DC Voltage, and Real and Reactive Power (RTDS sup capture #1 and 2)

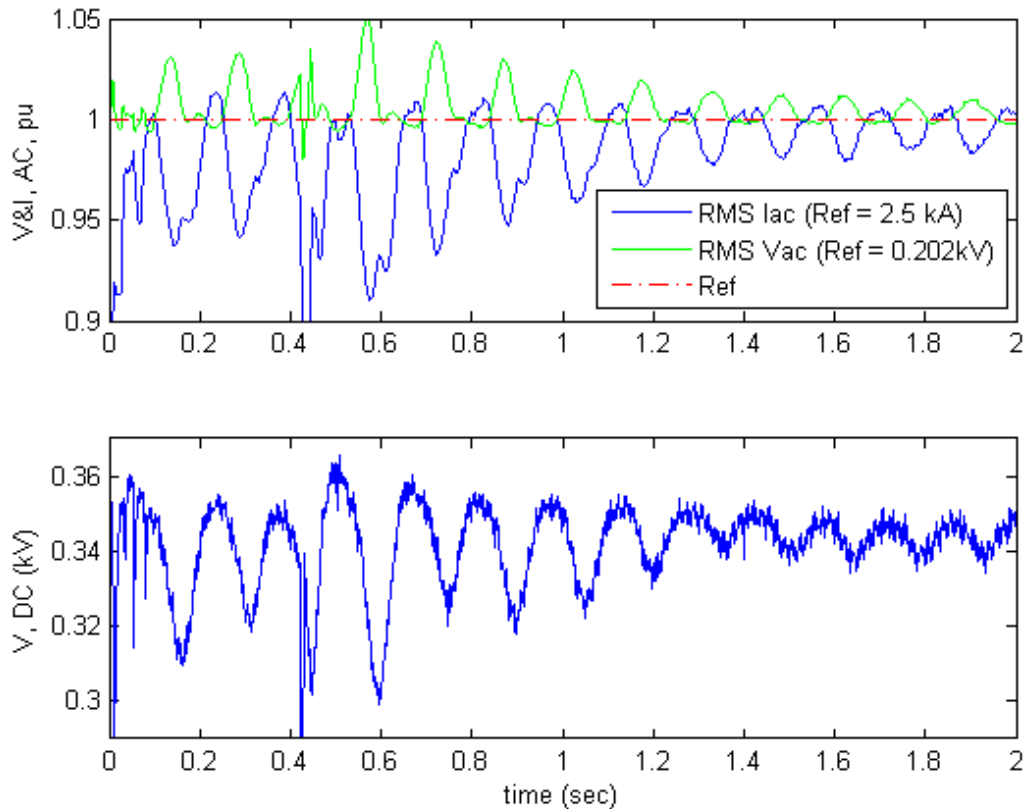


Figure 23: High-speed data capture of inverter AC voltage, AC current, and DC voltage, PHIL in open loop configuration (RTDS sup capture #3)

Based on the results of these and other data captures, we can make the following general observations:

1. Oscillations appear to occur somewhat regularly at 5-6 Hz.
2. The results of previous tests show that the inverter has some small, but visible variance in its real power output, even in the presence of a constant DC reference. This is due to the inverter's MPPT algorithm, which perturbs the DC link voltage to sense whether it is at the local optimum power point. As such, one would expect that, as the inverter approaches its power limit, these real power fluctuations would be accompanied by reactive power fluctuation such that the vector sum of real and reactive power is near constant. However, for prior tests (e.g., PF = 1.0, as presented in Section 3.1.3), these fluctuations are on the order of a few (1 to 2%) percent. In contrast, the observed fluctuations are up to 20% of the inverter's power rating. Thus, the surprising result from the test captures shown in Figure 19 and Figure 20 is not the presence of the fluctuations, but the *magnitude* of the oscillation.
3. The proximal reason for the decreases in real power is that the DC link voltage *decreases*, which indicates that the inverter's MPPT is actively curtailing the real power output. (Note that this is distinct from the reason for the transient decreases in power discussed in

Section 3.1.3, which were specifically connected to the DC link voltage *increasing* such that the voltage was on the low power side of the knee in the V-I curve). It is not immediately obvious why the DC voltage decreases.

4. The injection of reactive power has a significantly larger effect on the voltage at the inverter terminals than that seen in other tests. Specifically, as the reactive power becomes more negative, the voltage at the inverter terminals decreases, reaching as low as 0.95 pu (0.19 kV). Conversely, as the reactive power goes to zero, the voltage at the inverter terminals rise, reaching nearly 1.1 pu (0.22 kV). In addition, the effect of the reactive power on the voltage at the inverter terminals is considerably greater than that seen in other test runs. For example, Figure 23 compares the variation in voltage as a function of reactive power for the anomalous data capture (blue dots, -200 kVAr commanded, no power limit) with several test runs in which the inverter’s power factor command was varied (black dots); or in which reactive power was commanded, but for which the inverter’s power limit was set (green and red dots). The clustered blue dots (at -200 kVAr, ~0.2 kV) in the figure correspond to those points at which the inverter’s operation was stable, and are directly in line with the trend observed for other data captures. The scattered blue data points generally correspond to the periods in which oscillations were noted.

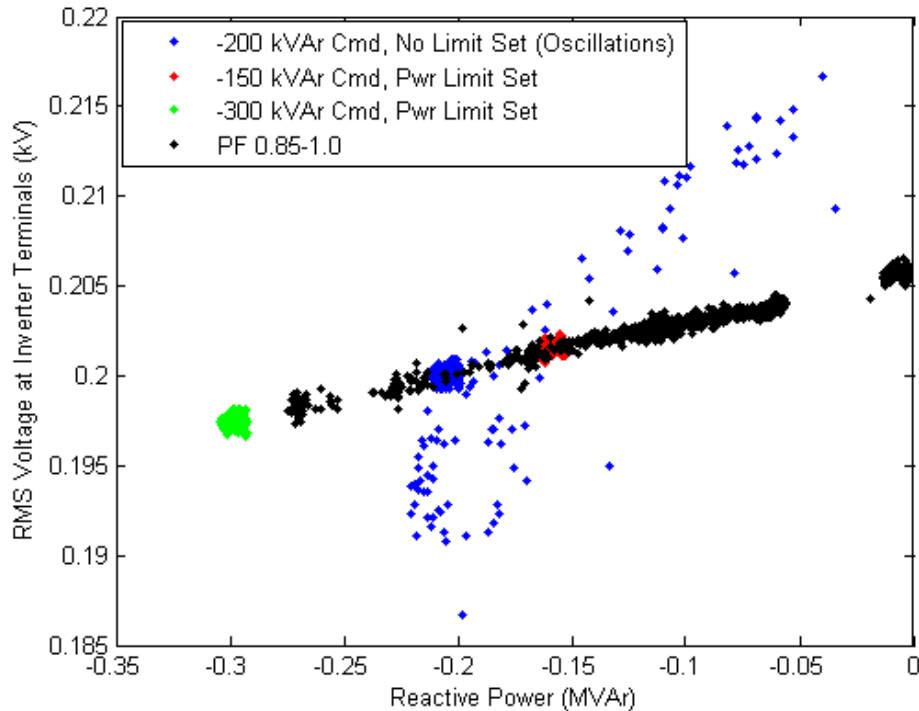


Figure 24: Comparison of inverter terminal voltage

6. Real power *increases* correlate with reactive power *decreases* (suggesting that the inverter is at or near a limit), but the inverter does not appear to ever actually reach 500 kVA (see fourth and fifth plots in Figure 20). However, the inverter does appear to hit a *current* limit of 2.5 kA (top plot in Figure 22 and Figure 21, note that the current, shown in blue, crosses the current limit, marked by the red dashed line) due to the low line voltage at high Q.

In general terms, then, a plausible explanation for the oscillation would go as follows:

1. The inverter's reactive power command pulls the inverter's terminal voltage low. As the inverter's real power increases, the inverter hits a current limit at a point somewhat below the inverter's power limit of 500 kVA (due to the low line voltage and the reactive power command, which requires a small, but non-zero, real current contribution).
2. The inverter responds immediately to the current limit by dropping its DC Voltage, as seen in the lower plots of Figure 22 and Figure 21, which has the immediate effect of reducing its real power output.
3. With the inverter's power limited, the inverter regulator *then* reduces its reactive power output (middle plot, blue line in Figure 21), which causes the AC line voltage to rise (top plot in Figure 22 and Figure 21, marked by the green line).
4. The rising line voltage allows the AC current to drop (so the inverter is no longer current limited). This, combined with the reduction in reactive power, offers additional head room for the real power to increase, and eventually, for the reactive power to increase as well.
5. Increasing reactive power again causes the line voltage to drop, and the cycle repeats itself.

The issue seems to hinge on: (1) the fact that the inverter's regulator seems to respond to a current limit first by reducing real power, then by reducing reactive power; (2) reducing the inverter's reactive power reduces the inverter's current output both directly (by reducing the total power output) and indirectly (by raising the line voltage). In combination, these effects appear to cause the inverter to over-compensate when it does reach a current limit.

It should be stressed that this is a preliminary analysis based on limited data, and requires additional investigation and testing to conclusively address the issue. In particular, it is not entirely clear what caused such wide variation in the voltage at the inverter terminals, particularly in light of the fact that, during the course of other tests, the inverter appears to have behaved differently under apparently similar operational conditions. It is also not clear whether the apparent delay in adjusting the inverter's reactive power is an artifact of the test configuration (e.g., the damping protection elements that were connected on the inverter's DC bus), or whether this reflects an actual limitation of the inverter's response.

4 Conclusions

Satcon conducted an independent review of the results of inverter power hardware in the loop (PHIL) tests of a 500 kVA Satcon PowerGate Plus operating in an emulated microgrid environment. The results tests were used to demonstrate operation of and gather data from the inverter in a simulated operational environment. In particular, testing demonstrated the ability of the inverter to operate in either a Power Factor Control Mode (constant power factor), or a Reactive Power Command Mode (constant reactive power), and to respond to real power limits.

Broadly speaking, analysis of the test results indicates that the test configuration appears to replicate real-world operation of a PV inverter, and that the tests successfully demonstrated operation of the inverter across a range of constant power factor commands, and a range of constant reactive power commands. Several issues surrounding the system's response to limit conditions were identified for further investigation during subsequent development or testing.

The PHIL test configuration appears to closely replicate real-world operation of a PV inverter: Under a baseline configuration in which the inverter's power factor was set to 1.0, the inverter's power output was shown to closely track the reference signal. Minor fluctuations in the inverter's DC input were shown to be consistent with operation of the inverter's MPPT algorithm and the V-I profile assumed for the emulated PV installation. Occasional transient errors in the inverter's DC input signal under high power operation were attributed to a delay in the DC VVS which caused the inverter's MPPT to drift into a low-power regime. The inverter's measured efficiency during testing tracks the inverter's rated CEC efficiency curve over its full range of power output. The measured efficiency was found to be systematically lower than the predicted efficiency by approximately 0.5% across the measured data points. We have speculated that this discrepancy is due to an unaccounted-for parasitic loss in the AC power measurement.

Demonstration of Power Factor Control Mode: The inverter was operated across a range of power factors from 0.85 to 1.0, inductive, over two different irradiance profiles. Consistent with expectations, the inverter's actual power factor was shown to closely track the commanded power factor. The error in the inverter's measured PF was typically well below 1% of its steady state value. Two minor issues were noted during testing, both of which we believe are artifacts of the test configuration:

- The inverter's actual PF shows a systematic error of approximately 1% compared to the commanded PF. This result would be consistent with an unaccounted for measurement error in the AC power output.
- Rapid changes in the system's real power output tend to correlate with errors of up to 3% in the inverter's actual PF. We have speculated that the protection elements on the inverter's DC bus, by limiting the inverter's ability to rapidly circulate power, slow its ability to rapidly change the reactive power output.

Demonstration of Reactive Power Command Mode: In Reactive Power Command Mode, the inverter was operated with constant reactive power commands of -150 and -300 kVAR over two different irradiance profiles. During these tests, the inverter's real power limit was configured such that the inverter would always have sufficient capacity to meet the reactive command. Analysis of the results showed that the inverter's reactive power output was within 2% of the

commanded level when the inverter remained below its kVA limit. As the inverter approached its kVA limit, this error increased to 5-10%. Measurements of the AC voltage at the inverter's terminals and the point of interconnect showed that the generation of reactive power has a measurable impact on the voltage of the distribution feeder in question, and that this effect is significantly larger for increasing plant size.

Oscillations in real and reactive power output when operating near the inverter's power limit: When operating near its power limits, the inverter exhibited oscillations in its real and reactive power output. Investigation of the available data suggests that the oscillations may be attributable to a lag in the inverter's curtailment of reactive power under limit conditions which was exacerbated by the effect of reactive power on the voltage at the inverter's terminals. It is not currently clear what caused the lag in the inverter's response or why the voltage at the inverter terminals showed such wide swings. These issues will be investigated in further tests.

Recommendations and Next Steps:

1. **PHIL Test Configuration:** The PHIL test environment offers a valuable tool to test inverter functionality in a controlled and flexible setting. To help facilitate data analysis, we would recommend that future PHIL tests include additional high speed data captures to help provide additional data as to the inverter's operating regime, and to help calibrate the data collection apparatus. The protection elements that were included in the test configuration may have had a minor impact on the test results, but are a critical element that should likely be included for future tests. We would recommend reviewing and monitoring the configurable voltage, current, and power limits to ensure that they are appropriate.
2. **Inverter Power Control Functions:** The inverter's Power Factor Control and Reactive Power Command Modes both function largely as expected. However, the observed oscillations in the inverter's real/reactive power output bear further investigation into the inverter controller's response under the specified conditions, as well as continued consideration of a yet-to-be-identified interaction with the test environment.

5 References

[1] B. Mather, J. Langston, K. Schoder, and F. Katiraei, “Power Hardware-In-Loop (PHIL) PV Inverter Testing,” Version 1.0, March 2012.